Dislocation Plasticity in Thin Metal Films

O. Kraft, L.B. Freund, R. Phillips, and E. Arzt

Abstract

This article describes the current level of understanding of dislocation plasticity in thin films and small structures in which the film or structure dimension plays an important role. Experimental observations of the deformation behavior of thin films, including mechanical testing as well as electron microscopy studies, will be discussed in light of theoretical models and dislocation simulations. In particular, the potential of applying strain-gradient plasticity theory to thin-film deformation is discussed. Although the results of all studies presented follow a "smaller is stronger" trend, a clear functional dependence has not yet been established.

Keywords: *mechanical properties, metals, thin films.*

Introduction

The behavior of thin metal films has been the subject of intense study over the past decade or more, driven largely by the importance of small-scale metal features in the fabrication and performance of microelectronic and optoelectronic devices, multilayer configurations for magnetic recording, and microelectromechanical systems (MEMS). It is primarily the electrical conductivity and chemical bonding characteristics of metals that are exploited in these applications. The low resistivity of aluminum and copper, along with techniques that have been developed for the deposition of patterned structures of these metals (lithographic processing technology), have put these particular materials in the research spotlight.

Although metals in the applications mentioned do not serve a load-bearing structural role, they are invariably subjected to high levels of mechanical stress as a result of the constraint on deformation imposed by other materials to which they are joined. Stress arises most commonly due to temperature change and is a consequence of the relatively high coefficients of thermal expansion of metals as compared with those of the semiconductors, glasses, and ceramics to which they are typically bonded. In general, metals under stress exhibit a propensity for inelastic deformation. At relatively low homologous temperatures, the physical mechanism giving rise to this inelastic deformation is predominantly dislocation nucleation and glide. Plastic deformation of a given material depends on many factors, including temperature, material microstructure, and material volume. It is the aim of this article to describe the current level of understanding of the mechanisms for plastic deformation in thin films and small structures, for which the connection between mechanical properties and material volume is a special characteristic. These issues are particularly important for assessing the reliability of metal structures integrated into small-scale systems during subsequent processing and long-term service.

Measuring Plastic Deformation

Because of the difficulties inherent in imposing stress on a thin film in a controlled way and in measuring film deformation, specialized techniques have been developed to study the mechanical behavior of films.[1–3] The configuration that has received the most attention is a metal film of nominally uniform thickness in the micrometer range deposited on and bonded to the flat surface of a substrate; usually, the substrate is relatively thick, compared with the film, and it has a relatively small coefficient of thermal expansion. In this case, stress can be imposed on the film by changing the temperature of the system.[4–18]

The constraint of the substrate implies that the generated thermal strain is essentially offset by the generation of some combination of elastic and plastic strain in the film. If σ is the equi-biaxial stress in the film, and ε_p is the equi-biaxial plastic strain, then rates of change are related by

$$\dot{\sigma}/M + \dot{\varepsilon}_p + (\alpha_{film} - \alpha_{sub})\dot{T} = 0,$$
$$\sigma(0) = \sigma_0, \qquad (1)$$

where α is a coefficient of thermal expansion. $M = E/(1 - \nu)$ is the biaxial elastic film modulus, where E is Young's modulus, and ν is the Poisson ratio. The temperature history $T(t)$ is presumed to be imposed, and σ_0 is the stress prior to temperature change.

Figure 1 illustrates stress evolution for two cases of Cu films deposited onto Si substrates with silicon nitride under layers as barriers to the diffusion of Cu into the substrate; the film thickness is 0.5 μm in both cases. In one case, the Cu film has a free surface, whereas in the other case it has a thin aluminum oxide layer on its surface; this layer was formed by self-passivation of a Cu-1at.%Al film.[19] After sputter-deposition of the films on their substrates and annealing at 600°C, the films are under tensile stress in excess of 400 MPa at room temperature; this defines the initial stress σ_0 in Equation 1. As the temperature is increased from room temperature, the film material tends to expand. It is constrained from doing so by the substrate, and in order to enforce this constraint, the stress in the film decreases linearly with increasing temperature. The slope of the curve is given by $(\alpha_{film} - \alpha_{sub})M$. At roughly 150°C, the film stress is zero, and upon further heating, the film stress becomes compressive. In this range, the behaviors of the free

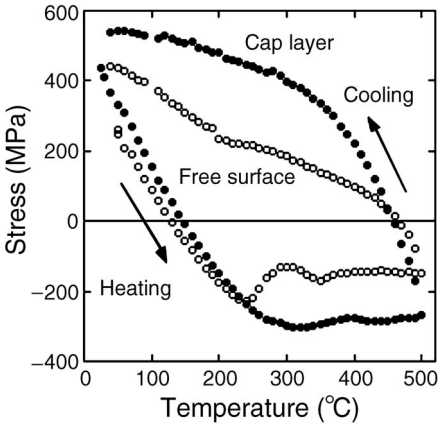

Figure 1. Stress-evolution as a function of temperature for Cu films with a thickness of 0.5 μm. The film stress was measured by the wafer-curvature technique (data from Reference 19). Solid circles (●) refer to a film with a cap layer, open circles (○) refer to a film with a free surface.

and passivated films are nearly identical. Eventually, the dependence of stress on temperature deviates from linear behavior, indicating the onset of plastic deformation. On cooling from the maximum temperature change of 500°C, the film tends to contract more than the substrate, and the initial slope is again the elastic slope. Consequently, the film stress changes from compression to tension and increases to more than 450 MPa when the temperature has been reduced to room temperature. However, the slope of the curves in the tensile-stress range is smaller than the thermoelastic slope, indicating that the film is being plastically deformed in the reverse direction in this range.

The stress in the passivated film is observed to be higher at comparable temperatures than in the unpassivated film throughout the regions of plastic straining. At temperatures higher than 300–400°C, this difference has been attributed to constrained diffusional creep via grain boundaries,[19] which is described in detail in the article by Josell et al. in this issue. Often, the stress–temperature evolution is regarded as a measure of film strength as a function of temperature; see, for example, Reference 7. However, this picture is incomplete, as the film stress relaxes quite substantially when temperature is held at a constant value; this tendency is more pronounced at the higher end of the temperature range being considered here.[8,18] Therefore, the rate of temperature change has an influence on the stress–temperature dependence observed, and the time-dependence of the plastic deformation needs also to be taken into account for a complete description. Furthermore, it has been discussed that the stress–temperature evolution is also influenced by strain-hardening or a Bauschinger effect[14,20,21] as the film is plastically strained, despite the fact that the imposed plastic strains of about 0.5% are rather small.

In the configuration just discussed, stress is induced in the film as a consequence of the constraint of the substrate when a thermoelastic mismatch strain is introduced in the film by a change in its temperature. Observations of the plastic response of thin films under direct tensile loading have also been reported for Ni,[22] Al,[23,24] Cu,[22,25] and multilayers.[26,27] Collectively, the data obtained support the view that the flow stress at a given level of plastic strain is higher in thin films than it is in chemically identical bulk samples and that flow stress usually increases with decreasing film thickness (or layer thickness in multilayers) and with decreasing grain size. The dependence on grain size is restricted to the temperature range for which plastic deformation is dominated by thermally activated glide of dislocations past lattice obstacles; the trend is reversed when the temperature is high enough for grain-boundary diffusion to contribute significantly to inelastic strain.[28]

There are some fundamental differences between experiments on freestanding films and on films bonded to thick substrates. An obvious difference is that freestanding films can be stressed only in tension but at fixed temperature, whereas films bonded to substrates with relatively low coefficients of thermal expansion can be stressed in both tension and compression but with varying temperature. A second, more subtle difference is that plastic deformation in the film is constrained kinematically by the substrate in the case of bonded films, but is not for freestanding films. Some possible implications of this difference will be addressed.

It has recently been demonstrated that the restriction to tensile stress in cases of direct mechanical loading can be overcome by depositing the thin metal film on a substrate that is elastically soft in comparison.[29] The stress–strain response of a Cu film that is 0.7 μm thick deposited on a polyimide substrate is shown in Figure 2. The stress was measured by *in situ* x-ray diffraction in this experiment. On loading, the film deforms first elastically until yielding at about 250 MPa is observed. Then, on straining to 0.5%, the flow stress increases to 400 MPa, indicating the presence of strain-hardening effects. On unloading of the specimen, the contracting elastic substrate compresses the film, which then undergoes plastic deformation in the opposite direction. It appears that on reverse loading, the yield strength is somewhat smaller compared with the initial loading, indicative of a Bauschinger effect.

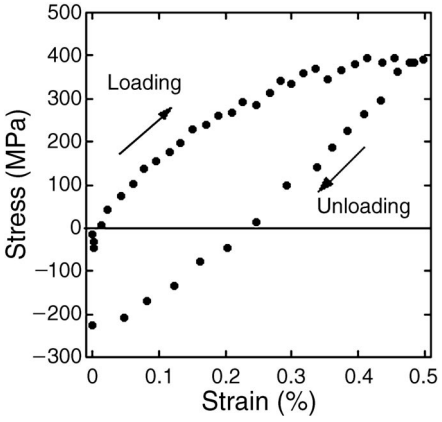

Figure 2. Stress-evolution as a function of applied strain for a Cu film with a thickness of 0.7 μm on a polyimide substrate. The film stress was measured by in situ *x-ray diffraction (data from Reference 29).*

Observation of Dislocation Motion

The behavior of an isolated dislocation on its glide plane in a stressed single-crystal thin film bonded to a substrate is illustrated schematically in Figure 3a for the case of a film with a free surface through which dislocations can leave the material. The driving force on the dislocation arises through the component of resolved shear stress on the glide plane acting in the direction of the Burgers vector of the dislocation. As the threading segment of the dislocation glides along through the film under the action of this driving force, it leaves behind an ever-increasing length of misfit dislocation on the film–substrate interface. The amount of plastic strain accumulated in this process is proportional to the total length of misfit dislocation. The same plastic strain is detected macroscopically for the case of many short segments as is detected for the case of a few long segments, provided only that the

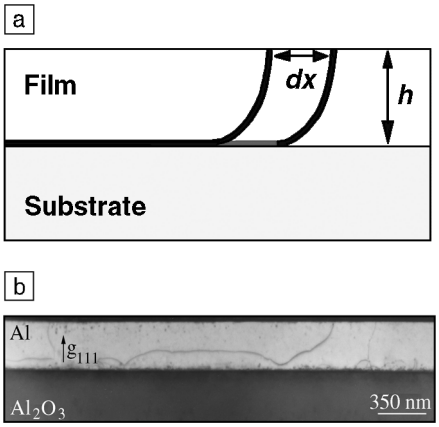

Figure 3. (a) Schematic representation of the motion of a single dislocation in a single-crystal film according to the model of Freund and Nix for a film with a free surface. It indicates that a dislocation segment with a length dx *needs to be created when the dislocation moves by* dx. *(b) Cross-sectional transmission electron micrograph showing a dislocation in a 350-nm-thick Al film, which was grown epitaxially on a (0001)-oriented Al_2O_3 substrate. Glide of a dislocation on the Al plane, which is inclined ~70° to the Al(111)‖Al_2O_3(0001) interface, created a dislocation segment nearly parallel to the interface. Contrast near the film–substrate interface indicates the presence of other, possibly misfit, dislocations. The diffraction vector is indicated by g_{111} (from Reference 31).*

total lengths are comparable. This mechanism has been observed in polycrystalline Al films with very large in-plane grain dimensions deposited on amorphous substrates[7] and in epitaxial Al films on Si[30] or Al_2O_3[31] substrates. A dislocation for which the threading segment has traveled a distance of several micrometers in the Al/Al_2O_3 system is shown in Figure 3b. The misfit segment is seen in the micrograph to stand off from the film–substrate interface by as much as 100 nm. The contrast variations close to the interface seen in Figure 3b suggest that the stand-off may be due to the stress fields of interface misfit dislocations that arrived at the interface earlier in time.

This picture of plastic-strain accumulation by the motion of threading dislocations on their glide planes can be generalized to account for other dislocations on parallel or intersecting glide planes, but all within the context of elastic homogeneity and planar glide. The uniformity of mechanical conditions along the glide plane necessary for this mode of relaxation is clearly not present in the case of polycrystalline thin films with a grain size of the order of the film thickness. In such a case, grain boundaries can serve as sources of dislocations as well as barriers to their motion. A goal for the field at the present time is to establish which physical mechanisms of plastic deformation are controlling the plastic response of the material for polycrystalline films. Kobrinsky and Thompson[18] have described dislocation motion in Ag films with thicknesses of about 200 nm and strongly textured microstructures at 150°C. Their *in situ* transmission electron microscopy (TEM) observations are consistent with the textbook picture of thermally activated dislocation glide, which leads to a jerky dislocation motion at low temperatures. The typical spacing between glide barriers and the typical glide distance from barrier to barrier were both reported to be between 50 nm and 100 nm. These distances are somewhat smaller than the film thickness or grain size, but by less than an order of magnitude. Similar TEM observations on polycrystalline Cu films on Si substrates with an intervening layer of amorphous SiN_x lead to the same general picture of plastic relaxation.[31,32] The typical dislocation distribution observed after heating to 600°C followed by cooling to 130°C is shown in Figure 4. For temperatures of less than 220°C, short segments of tangled dislocations and a jerky dislocation motion were observed, confirming the behavior reported by Kobrinsky and Thompson.[18] Collectively, these observations lend strong support to the hypothesis of thermally activated dislocation glide as the dominant plastic-deformation mechanism in these materials.

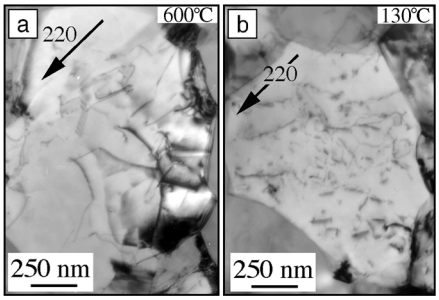

Figure 4. Dislocations in Cu grains at (a) 600°C and (b) 130°C. No interfacial dislocations deposited by advancing threading dislocations are discernible in the images. At elevated temperatures, (a) dislocations appear to be longer and more mobile than at lower temperatures (b), where dislocation motion became jerky and dislocation tangles formed. Plan-view transmission electron microscopy images are from Reference 32.

It was also pointed out by Dehm et al.[31] that no interfacial misfit dislocations were observed, which is at odds with the general notion of relaxation suggested in Figure 3 in which the film–substrate interface presents an impenetrable barrier to glide. If this is so, then dislocation lines should accumulate at such barriers in the course of plastic relaxation. *In situ* cross-sectional TEM observations also revealed that dislocations in the $Cu/SiN_x/Si$ system are attracted by the Cu/SiN_x interface, but again, no evidence of the interface misfit dislocations was found.[32] In contrast, Weihnacht and Brückner[33] and Shen et al.[21] observed interfacial dislocations in plan-view TEM and dislocation pile-ups in cross-sectional TEM for the $Cu/SiO_x/Si$ and Cu/SiO_x materials systems, respectively. This behavior appears to be connected to the quality of the interface bond; a model of a weak interface will be discussed.

Dislocations in Modeling

Discrete Dislocation Models

Freund[34] and Nix[1] have discussed the mechanics of glide of a single isolated threading dislocation in a single-crystal thin film, as depicted in Figure 3. As the threading segment of the dislocation glides through the film, it draws energy from the background elastic field arising from the applied or mismatch stress. The advancing dislocation leaves behind one interface misfit dislocation segment of increasing length, and the work expended in doing so imposes a retarding force on the threading dislocation. The yield strength τ_y is defined by the so-called Matthews–Blakeslee condition when the driving force and retarding force just balance each other. As a result, the yield strength varies with film thickness h roughly as h^{-1}.

The foregoing model is clearly not applicable in the case of polycrystalline films for which the underlying assumption of the steady advance of an isolated threading dislocation is precluded by the presence of grain boundaries. For polycrystalline films, Chaudhari[35] and Thompson[36] pointed out that if dislocations are confined to individual grains, then dislocation segments must be created at the grain boundaries as well as at the film–substrate interface. This leads to a flow-stress estimate that is proportional to h^{-1} for a fixed grain size and to D^{-1} for a fixed film thickness. It is noteworthy that this estimate, too, is based on the behavior of a single isolated dislocation. An experimental validation of these models based on the behavior of isolated dislocations has been given by Venkatraman and Bravman[7] for coarse-grained Al films and by Dehm et al.[31] for epitaxial thin Al films and Al_2O_3 substrates.

Plastic Rate Equations

For fine-grained polycrystalline films, on the other hand, these models tend to underestimate the yield strength, as was demonstrated by References 9, 14, 37, and 38, for example. This is not surprising, as many interacting dislocations are necessary to give rise to detectable levels of plastic deformation in fine-grained films. Under such conditions, the physical mechanism of plastic deformation is expected to be the thermally activated motion of dislocations past lattice obstacles, as it is for bulk samples of these materials, but with values of flow stress reflecting the special conditions that prevail in small-scale structures. This expectation was reflected in the early work of Flinn et al.[4] and Volkert et al.[8] on Al and Cu films, and it has been confirmed through direct observations by Kobrinsky and Thompson,[18] as noted earlier.

The theory of thermally activated glide of dislocations in fcc metals has its origins in statistical mechanics, but its implementation in continuum plasticity theory is largely empirical. A constitutive equation for dislocation motion on a particular glide system is customarily expressed in terms of an activation energy ΔF and a reference resolved shear stress $\hat{\tau}$ that by itself would induce the dislocation to bypass the obstacle if applied at zero absolute temperature T. The activation energy is a repulsive energy of interaction between a representative dislocation and an obstacle to glide in its path. The macroscopic plastic-strain

rate due to stress-assisted glide on that glide system is then expressed as

$$\dot{\gamma}_p = \dot{\gamma}_0 \exp\left[-\frac{\Delta F}{kT}\left(1 - \frac{|\tau|}{\hat{\tau}}\right)\right], \qquad (2)$$

where $\dot{\gamma}_0$ is a phenomenological constant, τ is the applied shear stress on the glide planes, k is the Boltzmann constant, and T is absolute temperature.

Once Equation 2 has been incorporated into Equation 1 by relating the shear on the glide systems to overall film strain and resolved shear stress to the biaxial film stress, it becomes an ordinary differential equation for stress as a function of time. Up to this point, the description of plastic deformation of a thin film includes no influence of deformation history on the instantaneous response to stress and temperature. This feature is often adopted on the basis of the behavior of films under cyclic stressing for which the response becomes cyclic after a small number of stress cycles. It has been pointed out by Shen et al.,[21] however, that there is persuasive evidence for deformation-history-dependence of response within each stress cycle. This history effect can arise principally in two ways. If a result of prior plastic deformation is to increase the number of obstacles to subsequent glide of dislocations in any shearing direction, the effect is viewed as isotropic strain-hardening, and it is included by considering $\hat{\tau}$ in Equation 2 to depend on plastic-strain history in some way. On the other hand, if a result of prior plastic deformation is to build up numbers of blocked dislocations in a certain direction of shearing, which can be released if the shearing direction is reversed, the effect is viewed as kinematic hardening, that is, hardening in one direction of stressing accompanied by softening in the opposite direction. It is included in constitutive modeling by referring stress to a nonzero "back stress" in some way. For a plastic rate equation of the form of Equation 2, the influence of kinematic hardening or back stress can be incorporated by referring the applied stress τ to a back stress τ_b that also depends on accumulated plastic strain.

Shen et al.[21] analyzed their data on temperature cycling of Cu films on silica substrates by appealing to the classical plasticity theory of kinematic hardening with a well-defined elastic range. Their general idea is also readily incorporated into the plastic rate equation framework, which preserves the connection to dislocation dynamics, by rewriting Equation 2 as

$$\dot{\gamma}_p = \dot{\gamma}_0 \exp\left[-\frac{\Delta F}{kT}\left(1 - \frac{|\tau - \tau_b|}{\hat{\tau}}\right)\right]. \qquad (3)$$

The particular form of back-stress-dependence on plastic strain introduced by Shen et al. was linear, essentially $\tau_b = \hat{\tau}\gamma_p/\gamma^*$, where a value of the parameter γ^* was deduced from the data.[21] The stress and strain parameters in Equation 3 can be interpreted as equivalent strain and effective stress parameters for isotropic response, or as resultant shear stress and shear strain on a particular slip system. In the latter case, τ_b would include self-hardening and latent hardening in different ways.

To illustrate the influence of the back-stress contribution, consider Equations 2 or 3 along with a simplified form of Equation 1 as $\dot{\tau}/G + \dot{\gamma}_p + \alpha\dot{T} = 0$ with $\tau(500°C) = 0$. Note that these differential equations now form a nonlinear coupled system of equations for $\tau(t)$ and $\gamma(t)$. Figure 5 shows that the behavior computed with this approach is, overall, in reasonable agreement with experimental data such as are shown in Figure 1. The influence of back stress is also illustrated in Figure 5, where the behavior leading to the two stress–temperature curves is identical except for the effect of the back stress (solid curve). The effect of the back stress leads to the commonly observed asymmetry in the magnitude of the stresses on heating and cooling. The high stresses, which are comparable to the experimental results, were obtained by adjusting $\hat{\tau}$ to about 250 MPa. Using Orowan's classical result, that the critical shear stress depends on the pinning-point distance L according to $\hat{\tau} = Gb/L$, where G is the shear modulus and b is the displacement distance, the corresponding pinning-point distance is 50 nm. This value is indeed much smaller than the film thickness and of the same order of magnitude as those observed by *in situ* TEM on Ag films by Kobrinsky and Thompson.[18] However, the approach presented here does not take into account that the pinning-point distance changes during heating and cooling (see Figure 4) as a result of strain-hardening and possibly recovery processes.

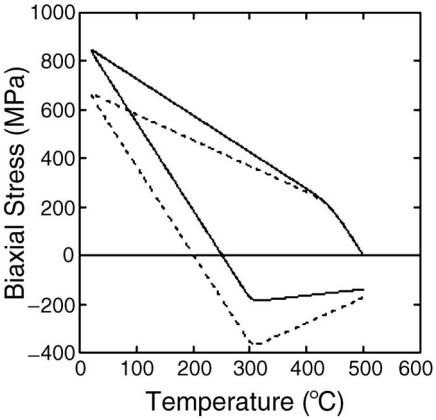

Figure 5. Stress versus temperature change for a film on a substrate, illustrating the difference between response according to the standard plastic rate equation (Equation 2, dashed curve) and a rate equation modified by the inclusion of a back stress depending on plastic strain (Equation 3, solid curve). Start with $\tau = 0$ was at 500°C; parameters used were for bulk Cu:[58] $\dot{\gamma}_0 = 1 \times 10^6\ s^{-1}$, $\Delta F = 3.5 \times 10^{-19}$ J. The Schmid factor s = 0.27 is for (111)-oriented grains; $\hat{\tau}$ was chosen to be 265 MPa and γ^* to be 0.005.

Strain-Gradient Plasticity

The discussion of continuum plasticity models for the deformation of thin metal films has been restricted up to this point to spatially homogeneous states of stress and strain. This is a natural consequence of the translationally invariant geometry of thin films and the absence of a length scale in the formulation. Motivated primarily by an accumulation of compelling observational evidence that such formulations are deficient, a search for a modified framework for describing plastic deformation in small volumes is being pursued actively. Experiments done with sample configurations as diverse as indentation (indentation sizes of 1–100 μm) and torsion of round wires (diameters of 10–200 μm) reveal a strong dependence of inferred flow stress on indentation size or wire diameter, mainly following the "smaller is stronger" trend.

The phenomenological strain-gradient plasticity theories are generalizations of classical continuum theories. The feature added is that the nonlinear relationship between stress and plastic strain at a point also involves the spatial gradient of plastic strain at that point.[39] The appearance of the strain gradient in the constitutive relation implies the existence of a characteristic length in the constitutive equations, thereby introducing a type of nonlocality. Furthermore, the appearance of the strain gradient leads naturally to couple stresses as force variables work-conjugate to the strain gradients. The predictions of this theory have been compared with available experimental data, and the characteristic length implied seems to fall in the range of 0.1–5 μm, well within the domain of thin-film plasticity.

Consider the deformation of a single crystal, large compared with atomic dimensions, due to dislocation motion on a single slip system. What is meant by

"plastic strain" of this material sample? Plastic deformation from an arbitrary initial configuration is a measure of the net number of dislocation lines that have passed completely through the sample, thereby altering the configuration. This number, along with the length of the Burgers vector, the geometry of the slip system, and the size of the sample, make it possible to identify a homogeneous, simple shear strain as a starting point for a continuum description of the process. In arriving at this description, there is no reference to dislocations remaining in the sample, but only to those passing completely through it. If the sample includes a random distribution of dislocations at the outset that does not change statistically during plastic straining, then the argument is unaffected and a homogeneous deformation can still be identified. On the other hand, if the Burgers circuit with dimensions on the scale of the sample size leads to a net offset that changes in the course of plastic deformation, then the interpretation as a homogeneous deformation becomes ambiguous. Furthermore, the situation becomes increasingly ambiguous as the sample size is made smaller. Finally, it is noted that some cases of plastic deformation require that a certain density of dislocations must be present for reasons of geometric compatibility; these are the so-called geometrically necessary dislocations introduced by Cottrell[40] and discussed by Ashby.[41]

The foregoing ideas underlie the development of strain-gradient plasticity theories. The reasoning is as follows: If some net density of dislocations is geometrically necessary in a particular plastically deforming crystal, then the deformation of a small sample of that material cannot be represented as being locally homogeneous. Instead, the deformation of a small sample also depends on the density of geometrically necessary dislocations, which is reflected macroscopically through a plastic-strain gradient. These ideas, which are discussed only loosely here, have been given a precise mathematical structure by Fleck and Hutchinson.[39] The structure of the theory, which continues to evolve, will not be discussed further here. Instead, some dislocation concepts on which it is based will be reviewed in the context of thin-film deformation.

Consider a single-crystal thin film subjected to an in-plane tensile stress. This stress is to be relaxed by symmetric double slip, that is, by glide of dislocations on symmetrically disposed glide planes. Strain-relieving dislocation loops are presumed to form at nucleation sites on the glide planes. These loops then expand, with one side passing out of the crystal through the free surface and the other side gliding toward the film–substrate interface, thereby resulting in elastic-strain relief. The ends of the loops form threading dislocations, which tend to move apart. The dislocation lines traveling toward the interface cannot penetrate the interface; the substrate is assumed to be very hard, compared with the film, and the interface boundary to be perfectly bonded for the time being. The first arriving dislocations are therefore blocked at the interface. Dislocations formed subsequently are repelled in their progress toward the interface by those arriving earlier, and dislocation pile-ups are formed, producing a back stress. Dislocation spacing in the pile-ups is smaller near the interface than it is further away. This deformation can be interpreted in terms of an effective extensional plastic strain $\varepsilon_p(y)$ in the direction parallel to the interface. This plastic strain is zero at the interface and increases with distance from the interface, with its gradient diminishing with distance from the surface. Loosely speaking, the gradient of plastic strain in the y direction is proportional to the local density of dislocations $\rho(y)$. Finally, for any finite level of stress, no dislocations can exist at points close to the free surface so that the density is zero there, which implies that the gradient of plastic strain vanishes at the surface, or $\varepsilon_p'(h) = 0$. An obvious implication of this simple line of reasoning is that the combination of an interface that is impenetrable to dislocations and the development of a dislocation pile-up due to the induced back stress leads to a plastic-strain distribution that necessarily varies through the thickness of the film.

How is this nonuniform strain distribution to be estimated, even in this simple case of symmetric double slip? From the perspective of dislocation mechanics, an additional strain-relieving dislocation can be inserted in a strained thin film whenever the interaction energy (of the dislocation with the equilibrium stress field existing prior to its formation) that is recovered balances the self-energy of formation. This is essentially an energy-minimization argument, so the same general approach might be adopted to determine $\varepsilon_p(y)$. In addition to the overall elastic energy for a given plastic strain with density $\frac{1}{2}M[\varepsilon_m - \varepsilon_p(y)]^2$, there is also a configurational energy stored in dislocation pile-ups. The closer together the dislocations are in a pile-up, the higher the value of this energy is. In effect, this pile-up results in an energetic penalty on the system for having closely spaced dislocations in its configuration that is not taken into account by macroscopic strain energy alone. Thus, an expression for energy per unit area incorporating such a penalty contribution is

$$W = \int_0^h \frac{1}{2} M([\varepsilon_m - \varepsilon_p(y)]^2 + \lambda^2 \varepsilon_p'(y)^2)\, dy, \qquad (4)$$

where λ is a material parameter with the dimensions of length that represents the sensitivity of the total energy to plastic-strain gradients. The measure W is now minimized if

$$\varepsilon_p(y) = \varepsilon_m\left(1 - \cosh\left(\frac{y}{\lambda}\right) + \sinh\left(\frac{y}{\lambda}\right)\tanh\left(\frac{h}{\lambda}\right)\right), \qquad (5)$$

which is the solution of a simple, ordinary differential equation obtained as a necessary condition for the minimizing strain distribution. This result satisfies the boundary conditions imposed on the basis of dislocation arguments, and it also reduces to the expected uniform strain result when $\lambda/h \to 0$. The foregoing discussion is intended to illustrate that plastic deformation can be spatially nonuniform in a material system for which it is commonly assumed to be uniform from the outset, that is, in a material system for which strain gradients may be an essential feature. This is done by appealing to only the most rudimentary aspects of the physics of plastic deformation.

Strain-gradient plasticity models have only recently been introduced into the discussion of plastic response of small material structures. This conceptual framework has the potential for providing quantitative predictions of the dependence of plastic-flow characteristics of small metal structures that arise from dislocation behavior, but without the need to confront the enormous complexity of the behavior of individual dislocations. While analysis of experimental data supporting the idea that plastic-strain gradients play an important role in small structures, film plasticity remains to be examined systematically from this point of view.

Weak Interface Effect

As has been noted, plastic deformation of a metal film consists largely of driving dislocations through the film toward the film–substrate interface. TEM observations of the interfaces of plastically deformed films show that interface dislocations are present in some cases, but not in others. It was also reported that interface dislocations disappear during TEM imaging.[42] In virtually all cases, the substrate material is

not deformed plastically, so the difference between these observations must be a consequence of variations in interface quality.

An interface that is fully or partially coherent will likely preserve the structure of nearby dislocations. In particular, the lattice distortion near the dislocation line that results in the contrast seen in TEM images will be preserved. If the interface is incoherent, on the other hand, its intrinsic resistance against slip can be much smaller than the flow strength of the film. Macroscopically, no traction is transmitted across the interface for a uniform film, and therefore the background film stress does not test the strength of the interface. In the case of a weak interface, the stress field of a dislocation near the interface, or perhaps of a group of similar dislocations, will result in a traction on the interface with the potential for inducing slip. The slip, in turn, softens the response detected by the dislocations to their environment and leads to an attractive force on the dislocations. Consequently, the configuration is unstable, and a dislocation is spontaneously drawn toward a weak interface. The range of the effect from the interface is roughly $Gb/2\pi\tau_0$, where τ_0 is the shear stress required to induce slipping on the interface. For $G = 100$ GPa, $b = 0.3$ nm, and $\tau_0 = 100$ MPa, this distance is about 50 nm.

The interaction between a dislocation and a weak interface is inherently nonlinear because the slipping zone at first expands as a dislocation is attracted to the interface. As the dislocation moves closer, the slipping zone necessarily contracts, leaving behind a slipped but no longer slipping portion. This nonlinear interaction has been described exactly within the framework of elastic dislocation theory by Hurtado and Freund.[43] The main consequence of the interaction is that the dislocations near weak interfaces are essentially drawn into the interface as slipping progresses. As a result, the large lattice distortions associated with dislocation cores give way to small lattice distortions over a relatively large part of the interface; the strain contrast of the core region is no longer seen in TEM observations, giving the impression that the dislocations have vanished. This is a possible explanation for the fact that interface misfit dislocations are not seen in some systems. Complete absorption of a dislocation by an interface requires minor atomic rearrangement at the interface, but this is quite possible, especially for an amorphous substrate material at elevated temperature. As pointed out in Reference 44, this behavior is reminiscent of the dislocation behavior in oxide-dispersion-strengthened materials, where the attraction of dislocations to the weak oxide/metal interface leads to the high-temperature strength of these materials.

Dislocation Simulation Studies

Analytical models for fundamental thin-film issues of dislocation interaction on parallel and intersecting glide planes have been discussed by Willis et al.[45] and Freund[46] and more recently in References 33 and 47. Even for such apparently simple configurations, the three-dimensional analyses are not immediately transparent. Consequently, substantial effort is being devoted to the development of computer-simulation methods, or so-called dislocation-dynamics methods, to understand multiple dislocation interactions both in thin films and in bulk materials. Schwarz[48,49] implemented the Peach–Koehler theory to simulate the motion and interaction of multiple dislocations in general three-dimensional strained heteroepitaxial film–substrate configurations. At an even more detailed level of modeling, interesting recent dislocation-dynamics simulations have also been undertaken, with the aim of examining plastic deformation induced in a metal film subject to indentation.[50]

As noted, the physics of both the nucleation and interaction of dislocations cannot be handled naturally in an elastic theory, and ad hoc rules were adopted for this purpose. To overcome some of the limitations of phenomenological plasticity models and of elastic-dislocation simulations, Phillips et al.[51] have studied atomistic models of the nucleation and interaction of dislocations that require no assumptions beyond those embodied in the interatomic potential. They emphasized the critical role of boundary conditions in simulating such events, and raised the important question of how more phenomenological simulation models can become better informed through atomistic modeling. From the standpoint of modeling dislocation-mediated plasticity in thin films, the key unknowns concern how to supplement the already convincing elastic analyses of the energetics of isolated dislocations with insights into the nucleation and interaction of such dislocations. An indication of the types of results that have been produced on the question of dislocation nucleation is illustrated in Figure 6, which shows dislocation loops nucleated in a molecular-dynamics calculation as a result of indentation.[52] Also, it is noted that Miller et al.[53] observed abundant dislocation nucleation at grain boundaries in an atomistic simulation of the advance of a crack in a grain of a polycrystal toward a grain boundary. Though such results indicate the basic mechanistic underpinnings for the deformation-induced nucleation of dislocations, a critical unresolved challenge remains the determination of systematic criteria for the nucleation of dislocations in thin films, as well as in the bulk.

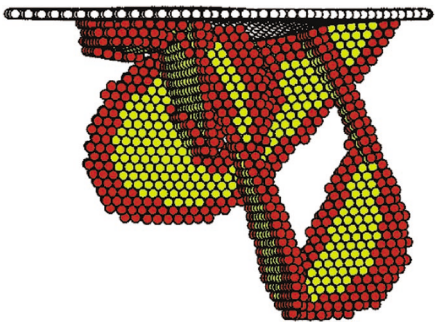

Figure 6. Illustration of the dislocation loops nucleated beneath an indenter, as computed using molecular dynamics (from Reference 52).

Pant et al.[54] adopted the approach of Schwarz to study specific dislocation interactions in fcc metal films on amorphous substrates. In contrast to epitaxial films, the film–substrate interface in this case is assumed to be impenetrable to dislocation motion. Many configurations of dislocations on parallel and intersecting glide planes with different combinations of Burgers vectors have been considered. It was found that the stress needed to drive a threading dislocation past an interface misfit dislocation in its path may be 30% larger than the stress needed to advance the isolated threading dislocation. For threading dislocations bypassing each other on parallel glide planes, the increase in flow stress is even stronger.

Interactions among large numbers of dislocations in a thin film under two-dimensional conditions have been simulated by Nicola et al.[55] for the case of a film with a free surface in tension and by Shu et al.[56] for the case of a film with passivated faces in simple shear. In the latter case, the problem was also modeled using strain-gradient plasticity. In both cases, strong gradients in plastic strain were found near boundary surfaces that are impenetrable to dislocation motion, similar to the behavior suggested by Equation 5. An example of a final equilibrium dislocation array in a film with a free surface obtained by Nicola et al. is shown in Figure 7.

A discrete dislocation simulation model for the study of film plasticity at the level of a single grain has been developed by von Blanckenhagen et al.,[57] also within the framework of isotropic linear elasticity. All boundaries of the columnar grain, includ-

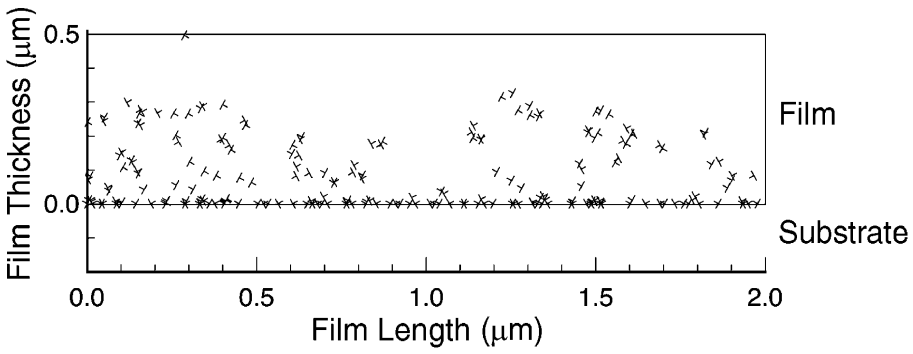

Figure 7. Dislocation distribution as calculated by two-dimensional dislocation dynamics in a 0.5-μm-thick Al film after cooling by 300 K (from Reference 55).

ing the lateral grain boundaries and the interface with the substrate and the passivated surface, are assumed to be impenetrable to dislocations. The generation of dislocations by a Frank–Read source within the grain and the formation of the pile-ups on the glide planes were simulated. The optimal size of the source was found to be between one-fourth and one-third of the smallest grain dimension. Because the stress required to activate the source scales with source size, this implies a strong connection between plastic-flow stress and microstructural dimensions. The effect of source size also decreases as the number of dislocations produced increases. The result that the dislocation source size scales with the smaller grain dimension, either the film thickness or the in-plane grain size, implies that a critical microstructural size exists below which the flow stress depends on the inverse grain size instead of on the square root of this dimension.

This simulation has been extended recently to take into account a distribution of potential Frank–Read sources. A strain is imposed on the grain, and the evolution of stress, plastic strain, and dislocations are calculated. As an example of such a simulation, Figure 8 shows the dislocation configuration in an fcc grain of width 512 nm after it was plastically strained up to 0.12%. A parallel dislocation array (PDA) and a pile-up (PU) of dislocations at the interface with the substrate can be readily identified. Furthermore, tangled dislocations (T) and dislocation sources (DS) that bow out without producing a full dislocation loop are also evident. These dislocation configurations lead to a strong increase in flow stress as a function of plastic strain, and the predicted stresses are even higher than those measured experimentally for a comparable situation (see, e.g., Figure 2). This is plausible, however, because the simulation does not include any processes like cross-slip, dislocation core-spreading, or other relaxation mechanisms.

Concluding Remarks

All studies presented and discussed here indicate clearly that the motion of dislocations is constrained in thin metal films, due to the reduced material volume, the presence of the interfaces to a substrate, and/or passivation. As a result, the mechanical behavior of thin metal films can be qualitatively summarized by saying that *smaller is stronger.* Up to now, however, a clear functional dependence had not been established, either empirically or theoretically. This ambiguity is further accentuated by the fact that the grain size of polycrystalline films as well as subtle changes in the chemistry of the interfaces present play an important role for dislocation plasticity in thin films. The general area would benefit from greater emphasis on understanding how individual dislocations interact with or are generated from physically realistic grain boundaries and incoherent interfaces. This will require

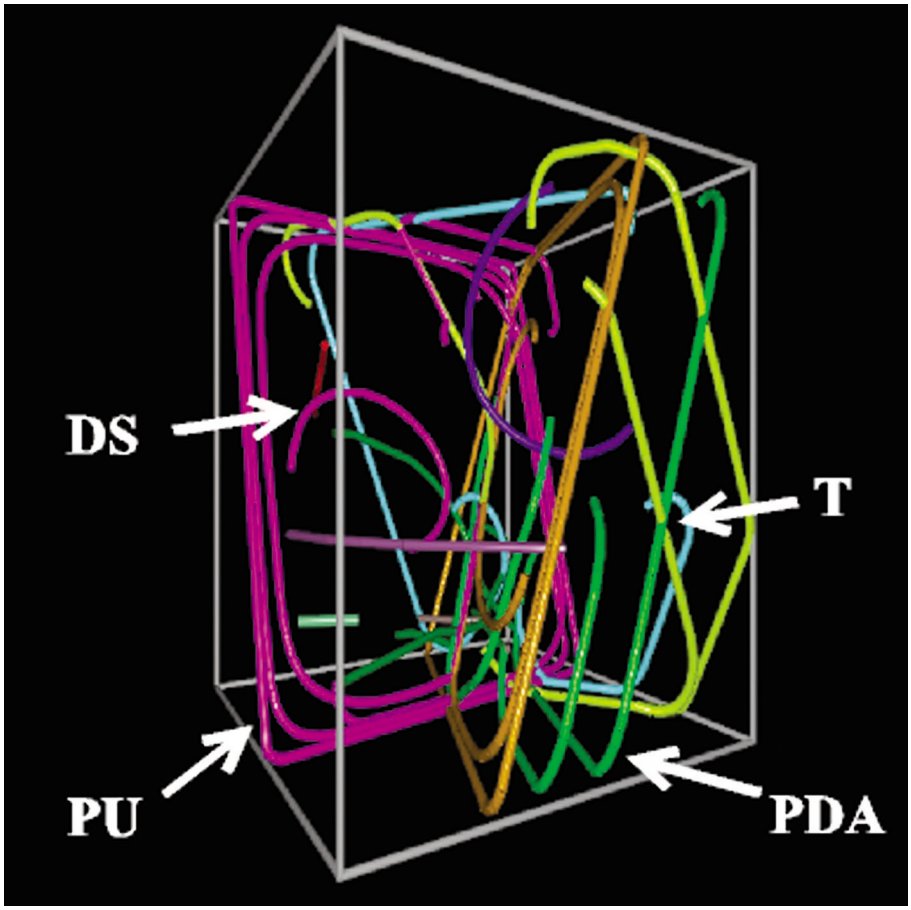

Figure 8. Dislocation distribution as calculated by three-dimensional dislocation dynamics in a 512-nm cubic grain.[59] The simulation was conducted as described in Reference 57; the interfaces and grain boundaries were assumed to be impenetrable for dislocations, and the parameters used were for Cu. DS is a dislocation source, T is a tangled dislocation, PDA is a parallel dislocation array, and PU is a pile-up of dislocations.

fairly extensive simulation studies and will rely on insight and judgment in problem definition. For the latter, a vivid exchange between experiments—including mechanical testing as well as *in situ* electron microscopy—and theory is indispensable.

Owing to the constraints on dislocation motion, dislocation plasticity is strongly reduced as a stress-relaxation mechanism. Thus, very high internal stresses may be present in small-scale devices and endanger operation. Continuum theories of plasticity that incorporate a physical or microstructural length scale may turn out to be very helpful if they can be shown to have a predictive capability. Such a theory may be based on strain-gradient plasticity, which shows great promise, but needs to prove applicability to deformation in thin metal films. If such theories are guided by experiments and able to capture the essence of the response of small structures, they will be very useful in device simulation codes for microelectronics, MEMS, and other applications.

References

1. W.D. Nix, *Metall. Trans. A* **20A** (1989) p. 2217.
2. F.R. Brotzen, *Int. Mat. Rev.* **39** (1994) p. 24.
3. O. Kraft and C.A. Volkert, *Adv. Eng. Mater.* **3** (2001) p. 99.
4. P.A. Flinn, D.S. Gardner, and W.D. Nix, *IEEE Trans. Electron Devices* **ED-34** (1987) p. 689.
5. P.A. Flinn and C. Chiang, *J. Appl. Phys.* **67** (1990) p. 2927.
6. P.A. Flinn, *J. Mater. Res.* **6** (1991) p. 1498.
7. R. Venkatraman and J.C. Bravman, *J. Mater. Res.* **7** (1992) p. 2040.
8. C.A. Volkert, C.F. Alofs, and J.R. Liefting, *J. Mater. Res.* **9** (1994) p. 1147.
9. R.P. Vinci, E.M. Zielinski, and J.C. Bravman, *Thin Solid Films* **262** (1995) p. 142.
10. S. Bader, P.A. Flinn, E. Arzt, and W.D. Nix, *J. Mater. Res.* **9** (1994) p. 318.
11. S. Bader, E.M. Kalaugher, and E. Arzt, in *Thin Films: Stresses and Mechanical Properties V,* edited by S.P. Baker, C.A. Ross, P.H. Townsend, C.A. Volkert, and P. Børgesen (Mater. Res. Soc. Symp. Proc. **356**, Pittsburgh, PA, 1995) p. 435.
12. P.R. Besser, S. Brennan, and J.C. Bravman, *J. Mater. Res.* **9** (1994) p. 13.
13. M.A. Moske, P.S. Ho, D.J. Mikalsen, J.J. Cuomo, and R. Rosenberg, *J. Appl. Phys.* **74** (1993) p. 1716.
14. R.-M. Keller, S.P. Baker, and E. Arzt, *J. Mater. Res.* **13** (1998) p. 1307.
15. R.-M. Keller, S.P. Baker, and E. Arzt, *Acta Mater.* **47** (1999) p. 415.
16. O. Kraft and W.D. Nix, in *Materials Reliability in Microelectronics VIII,* edited by J.C. Bravman, T.N. Marieb, J.R. Lloyd, and M.A. Korhonen (Mater. Res. Soc. Symp. Proc. **516**, Warrendale, PA, 1998) p. 201.
17. M.J. Kobrinsky and C.V. Thompson, *Appl. Phys. Lett.* **73** (1998) p. 2429.
18. M.J. Kobrinsky and C.V. Thompson, *Acta Mater.* **48** (2000) p. 625.
19. D. Weiss, H. Gao, and E. Arzt, *Acta Mater.* **49** (2001) p. 2395.
20. M. Ronay, *Philos. Mag. A* **40** (1979) p. 145.
21. Y.-L. Shen, S. Suresh, M.Y. He, A. Bagchi, O. Kienzle, M. Rühle, and A.G. Evans, *J. Mater. Res.* **13** (1998) p. 1928.
22. J.A. Ruud, D. Josell, F. Spaepen, and A.L. Greer, *J. Mater. Res.* **8** (1993) p. 112.
23. D.T. Read and J.W. Dally, *J. Mater. Res.* **8** (1993) p. 1542.
24. G. Cornella, R.P. Vinci, R. Suryanarayanan Iyer, R.H. Dauskardt, and J.C. Bravman, in *Microelectromechanical Structures for Materials Research,* edited by S. Brown, J. Gilbert, H. Guckel, R. Howe, G. Johnson, P. Krulevitch, and C. Muhlstein (Mater. Res. Soc. Symp. Proc. **518**, Warrendale, PA, 1998) p. 81.
25. D.T. Read, *Int. J. Fatigue* **20** (1998) p. 203.
26. D. Josell, D. van Heerden, D. Read, J. Bonevich, and D. Shechtman, *J. Mater. Res.* **13** (1998) p. 2902.
27. H. Huang and F. Spaepen, *Acta Mater.* **48** (2000) p. 3261.
28. M.D. Thouless, J. Gupta, and J.M.E. Harper, *J. Mater. Res.* **8** (1993) p. 1845.
29. M. Hommel, O. Kraft, and E. Arzt, *J. Mater. Res.* **14** (1999) p. 2373.
30. E.A. Stach, U. Dahmen, and W.D. Nix, in *Recent Developments in Oxide and Metal Epitaxy—Theory and Experiment,* edited by M. Yeadon, S. Chiang, R.F.C. Farrow, J.W. Evans, and O. Auciello (Mater. Res. Soc. Symp. Proc. **619**, Warrendale, PA, 2000) p. 27.
31. G. Dehm, B.J. Inkson, T.J. Balk, T. Wagner, and E. Arzt, in *Dislocations and Deformation Mechanisms in Thin Films and Small Structures,* edited by O. Kraft, K.W. Schwarz, S.P. Baker, L.B. Freund, and R. Hull (Mater. Res. Soc. Symp. Proc. **673**, Warrendale, PA, 2001) p. P2.6.1.
32. G. Dehm, D. Weiss, and E. Arzt, *Mater. Sci. Eng., A* **309–310** (2001) p. 468.
33. V. Weihnacht and W. Brückner, *Acta Mater.* **49** (2001) p. 2365.
34. L.B. Freund, *J. Appl. Mech.* **43** (1987) p. 553.
35. P. Chaudhari, *Philos. Mag. A* **39** (1979) p. 507.
36. C.V. Thompson, *J. Mater. Res.* **8** (1993) p. 237.
37. S.P. Baker, A. Kretschmann, and E. Arzt, *Acta Mater.* **49** (2001) p. 2145.
38. M. Hommel and O. Kraft, *Acta Mater.* **49** (2001) p. 3935.
39. N.A. Fleck and J.W. Hutchinson, *Adv. Appl. Mech.* **33** (1997) p. 295.
40. A.H. Cottrell, *The Mechanical Properties of Matter* (John Wiley & Sons, New York, 1964).
41. M.F. Ashby, *Philos. Mag.* **21** (1970) p. 399.
42. P. Müllner and E. Arzt, in *Thin Films: Stresses and Mechanical Properties VII,* edited by R.C. Cammarata, M. Nastasi, E.P. Busso, and W.C. Oliver (Mater. Res. Soc. Symp. Proc. **505**, Warrendale, PA, 1998) p. 149.
43. J.A. Hurtado and L.B. Freund, *J. Elasticity* **52** (1999) p. 167.
44. E. Arzt, G. Dehm, P. Gumbsch, O. Kraft, and D. Weiss, *Prog. Mater. Sci.* **46** (2001) p. 283.
45. J.R. Willis, S. Jain, and R. Bullough, *Appl. Phys. Lett.* **59** (1991) p. 920.
46. L.B. Freund, *Advances in Applied Mechanics,* Vol. 30 (Academic Press, New York, 1993).
47. W.D. Nix, *Scripta Mater.* **39** (1998) p. 545.
48. K.W. Schwarz, *J. Appl. Phys.* **85** (1999) p. 108.
49. K.W. Schwarz, *J. Appl. Phys.* **85** (1999) p. 120.
50. C.F. Robertson and M.C. Fivel, *J. Mater. Res.* **14** (1999) p. 2251.
51. R. Phillips, D. Rodney, V. Shenory, E. Tadmor, and M. Ortiz, *Model. Simul. Mater. Sci. Eng.* **7** (1999) p. 769.
52. C.L. Kelchner, S.J. Plimpton, and J.C. Hamilton, *Phys. Rev. B* **58** (1998) p. 11085.
53. R. Miller, E.B. Tadmor, R. Phillips, and M. Ortiz, *Model. Simul. Mater. Sci. Eng.* **6** (1998) p. 607.
54. P. Pant, K.W. Schwarz, and S.P. Baker, in *Dislocations and Deformation Mechanisms in Thin Films and Small Structures,* edited by O. Kraft, K.W. Schwarz, S.P. Baker, L.B. Freund, and R. Hull (Mater. Res. Soc. Symp. Proc. **673**, Warrendale, PA, 2001) p. P2.2.1.
55. L. Nicola, E. van der Giessen, and A. Needleman, *Mater. Sci. Eng. A* **309–310** (2001) p. 274.
56. J.Y. Shu, N.A. Fleck, E. van der Giessen, and A. Needleman, *J. Mech. Phys. Solids* **49** (2001) p. 1361.
57. B. von Blanckenhagen, P. Gumbsch, and E. Arzt, *Model. Simul. Mater. Sci. Eng.* **9** (2001) p. 157.
58. H.J. Frost and M.F. Ashby, *Deformation-Mechanism Maps: The Plasticity and Creep of Metals and Ceramics* (Pergamon Press, New York, 1982).
59. B. von Blanckenhagen (unpublished results).

□